ELSEVIER

Biochimica et Biophysica Acta 1194 (1994) 53–60

BBA Biochimica et Biophysica Acta

Interaction of cord factor (α,α'-trehalose-6,6'-dimycolate) with phospholipids

L.M. Crowe [a,*], B.J. Spargo [a,b], T. Ioneda [c], B.L. Beaman [d], J.H. Crowe [a]

[a] *Section of Molecular and Cell Biology, University of California, Davis, CA 95616, USA*
[b] *Center for Bio / Molecular Science and Engineering, Naval Research Laboratories, Washington, DC 20375, USA*
[c] *Department of Microbiology, University of Sao Paulo, Sao Paulo, Brazil*
[d] *Department of Medical Microbiology and Immunology, University of California, Davis, CA 95616, USA*

Received 3 March 1994

Abstract

We previously reported that cord factor (α,α'-trehalose-6,6'-dimycolate) isolated from *Nocardia asteroides* strain GUH-2 strongly inhibits fusion between unilamellar vesicles containing acidic phospholipid. We chose to study the effects of this molecule on liposome fusion since the presence of *N. asteroides* GUH-2 in the phagosomes of mouse macrophages had been shown to prevent phagosomal acidification and inhibit phagosome-lysosome fusion. A virtually non-virulent strain, *N. asteroides* 10905, does not prevent acidification or phagosome-lysosome fusion and, further, contains only trace amounts of cord factor. In the present paper, we have investigated the effects of cord factor on phospholipid bilayers that could be responsible for the inhibition of fusion. We show that cord factor increases molecular area, measured by isothermal compression of a monolayer film, in a mixed monolayer more than would be expected based in its individual contribution to molecular area. Cord factor, as well as other glycolipids investigated, increased the overall hydration of bilayers of dipalmitoylphosphatidylcholine by 50%, as estimated from the unfrozen water fraction measured by differential scanning calorimetry. The effect of calcium on this increased molecular area and headgroup hydration was measured by fluorescence anisotropy and FTIR spectroscopy of phosphatidylserine liposomes. Both techniques showed that cord factor, incorporated at 10 mol%, increased acyl chain disorder over controls in the presence of Ca^{2+}. However, FTIR showed that cord factor did not prevent headgroup dehydration by the Ca^{2+}. The other glycolipids tested did not prevent either the Ca^{2+}-induced chain crystallization or headgroup dehydration of phosphatidylserine bilayers. These data point to a possible role of the bulky mycolic acids of cord factor in preventing Ca^{2+}-induced fusion of liposomes containing acidic phospholipids.

Key words: Trehalose dimycolate; Liposome fusion; Phosphatidylserine; DSC; FTIR; Bilayer hydration

1. Introduction

Pathogenic bacteria such as *Mycobacterium tuberculosis, M. microti, M. avium* and *Nocardia asteroides* have been shown to inhibit or prevent fusion of lysosomes with bacteria-containing phagosomes in macrophages [1–6]. Methods used to detect inhibition of phagosome-lysosome fusion included labeling of lysosomes with acridine orange, and the fusion with phagosomes evaluated by light microscopy. In addition, phagosome-lysosome fusion using electron dense labels such as ferritin, peroxidase, and acid phosphatase histochemistry has been evaluated with electron microscopy [1–3,5–7]. Even though Goren suggested [6] that acridine orange is not specific for this purpose, numerous investigators have included electron microscopic evidence using electron dense labels as described above to confirm the results based on acridine orange labeling experiments.

Abbreviations: DMPS, dimyristoylphosphatidylcholine; DPH, diphenylhexatriene; DPPC, dipalmitoylphosphatidylcholine; DSC, differential scanning calorimetry; CF, cord factor; FTIR, Fourier transform infrared spectroscopy; MLV, multilamellar vesicles; POPA, palmitoyloleoylphosphatidic acid; PS, top fraction bovine brain phosphatidylserine; TEC-Mal, triethoxycholesterol maltose; Tes, *N*-tris(hydroxymethyl)methyl-2-aminoethanesulfonic acid; TDB, trehalose dibehenate (didocosanoyl trehalose); T_m, gel-to-liquid crystalline transition temperature.

* Corresponding author. Fax: +1 (916) 7521094.

SSDI 0005-2736(94)00121-5

The mechanism by which phagosome-lysosome fusion is inhibited is not clear. Goren et al. [2] suggested that a molecule from the cell wall of *M. tuberculosis*, a polyanionic sulfoglycolipid called SL-1 or 2,3,6,6′-tetracyl trehalose 2′-sulfate [10], may be involved. Phagosome-lysosome fusion in macrophages was inhibited when the SL-1 was present in the lysosomes (via uptake of an emulsion) or in the phagosomes (via uptake of SL-1 coated yeast cells). Goren et al. [8], later suggested that polyanions, as a general class of substances, appear to inhibit phagosome-lysosome when sequestered in the lysosomal compartment, but he believed this to be an artifactual result. The authors specifically exclude the mycobacterial sulfolipid polyanions, which they state require further study. There is some disagreement with this point of view [9]. These doubts concerning artifactual results, however, do not appear to apply to studies in which electron dense markers (e.g., ferritin) are sequestered in the lysosomes in the absence of polyanions and the mycobacteria are present in the phagosome. Experiments cited above [2] in which phagosome-lysosome fusion is inhibited when SL-1 coated yeast cells are in the phagosome suggest that this mycobacterial sulfoglycolipid may play a role. However, it is important to note that a variety of mycolic acid-containing bacteria such as *Rhodococcus* and *Nocardia* inhibit phagosome-lysosome fusion in macrophages; yet, they do not possess detectable amounts of the sulfoglycolipid SL-1.

There is at least one study that indicates that host cell characteristics play a role in the inhibition of *M. avium* -containing phagosomes [7]. Macrophages from bacterial-resistant and bacterial-sensitive mice show large differences in the amount of phagosome-lysosome fusion when infected with the same virulent strain as determined by the use of staining of acid phosphatase as a fusion marker [7]. Most recently, it has been shown that phagosomes containing *M. avium* do not acidify normally and that this is due to the lack of a proton-ATPase [11] in the phagosomal membrane. The evidence available does not allow differentiation between inhibition of fusion with proton-ATPase-carrying vesicles or rapid removal of proton-ATPase complexes from the phagosomes. Similarly, it was shown previously that live or killed *N. asteroides* GUH-2 blocks completely phagosomal acidification following phagocytosis by macrophages [12]. In contrast, avirulent strains of *N. asteroides* do not inhibit phagosomal acidification [12].

In the case of *N. asteroides*, the presence of cord factor (α,α'-trehalose-6,6′-dimycolate) is implicated in toxicity [13] and the inhibition of fusion [3]. The virulent strain, *N. asteroides* GUH-2, had 3 to 4-times as much glycolipid (of which 95% was identified as authentic cord factor) as the relatively non-virulent strain *N. asteroides* 10905 in which only trace amounts of cord factor were detectable [13]. The composition and toxicity of lipid fractions from these two strains have been determined [13] and the mycolic acids of GUH-2 have been characterized [14]. The most abundant mycolic acid in this strain is $C_{52:2}$, and chain lengths range from C_{50} to C_{54}.

Recently, we reported that CF from strain GUH-2, when incorporated into the bilayers at 10 mol%, markedly inhibited Ca^{2+}-induced fusion of large unilamellar vesicles containing acidic phospholipids [15]. In light of reports indicating that Ca^{2+} dehydrates the phosphate of the headgroup, rigidifies the acyl chains, and bridges acidic phospholipids between bilayers [16–26] we suggested that CF inhibits fusion in this model membrane by increasing the hydration and fluidity of the membrane. These two factors may not be independent of each other: for example increased fluidity could come about because of increased molecular area due to head-group size, head-group hydration, or by decreased chain packing due to bulky mycolic acids. Conversely, decreased chain packing could lead to increased molecular area and head-group hydration. An increase in the hydration of the membrane could inhibit Ca^{2+}-induced dehydration; increased bilayer fluidity might decrease the possibility of packing defects suggested to result in fusion [27]. Further, increased hydration could lead to an increase in the hydration force which prevents the close approach of bilayers, a requirement for fusion [27,28]. In the present study we examine the hydration, molecular area, and fluidity of model lipids in the presence of cord factor.

2. Materials and methods

Palmitoyloleoylphosphatidic acid (POPA), top fraction crude bovine brain phosphatidylserine (PS), dimyristoylphosphatidylserine (sodium salt) (DMPS), dimyristoylphosphatidylcholine (DMPC) and dipalmitoylphosphatidylcholine (DPPC) were obtained from Avanti Polar Lipids (Alabaster, AL) and used without further purification. Trehalose dibehenate (TDB) was obtained from Sigma (St. Louis, MO). Lipids were stored in chloroform at −20°C. Lipid purity was checked in various experiments by thin layer chromatography or differential scanning calorimetry with results consistent with high lipid purity. Triethoxycholesterol maltose (TEC-Mal) was a generous gift from Raymond P. Goodrich [29]. 1,6-Diphenyl-1,3,5-hexatriene (DPH) was obtained from Molecular Probes (Eugene, OR). Cord factor (CF) was purified from *Nocardia asteroides*, strain GUH-2 and was checked for purity and molecular mass using direct-inlet HPLC-MS (Hewlett-Packard, Concord, CA). Water used for the monolayer experiments was HPLC grade obtained from Fisher. For the other experiments, water was purified

with Barnstead columns to remove organics and ions and provided a resistivity of at least 14 Mohm/cm.

2.1. Thin-layer chromatography

Lipids and lipid mixtures were spotted on HPTLC or preparative silica gel plates (Merck, Darmstadt, Germany) along with authentic lipid standards and run in chloroform/methanol/water (65:35:5, v/v) [30]. Lipids were visualized with iodine vapor or charring, or in the case of glycolipids with an α-napthol reagent [30].

2.2. Preparation of lipids and liposomes

For the various experiments, aliquots of lipid were dried in clean, pre-weighed glass tubes under a stream of nitrogen, then kept at high vacuum overnight to remove residual chloroform. Components of lipid mixtures were dried and weighed separately, then redissolved in chloroform, aliquots were mixed to give the appropriate mol ratios, then redried. For the monolayer experiments, the lipid was re-dissolved in the appropriate solvent at a concentration of 1 mg/ml.

For the preparation of multilamellar vesicles (MLV), the thin film of lipid in the glass tube was hydrated by the addition of water or buffer, incubated above T_m for at least 5 min, then vortexed. This cycle was repeated several times until all the lipid was suspended. All liposomes were prepared in excess water or buffer.

Unilamellar vesicles were prepared by modification of the ether vaporization method of Deamer [31]. Briefly, an ether emulsion of lipid was injected into buffer at 70°C, and the resulting liposomes were extruded through two stacked polycarbonate 0.2 μm filters at approximately 3.5 MPa of N_2.

2.3. Monolayer films

Films of the lipids were cast at 1 mg/ml in hexane with the exception of DMPC and mixtures containing DMPC which were cast from hexane/chloroform (9:1, v/v). The subphase consisted of 10 mM Tes, 100 mM NaCl (pH 7.5) which had been passed through a 0.2 μm nylon filter prior to use. Before each compression, the subphase was tested for surface activity by compression of the barrier: no surface activity was found. The 5.0×7.0 cm trough and the barrier were milled from Teflon, and the trough was fixed to a stainless steel base through which water circulated to maintain temperature. The movable barrier was regulated by a stepping motor under analog control.

The surface pressure was measured continuously with a 2.0 cm perimeter platinum Wilhelmy plate suspended from the beam of a Cahn Electrobalance and recorded by a chart recorder calibrated to 80 mN/m full scale. Isothermal measurements were made at 30°C: the temperature was continuously monitored with a thermocouple submerged in the subphase outside the film area. The barrier was advanced at 0.5 cm/min after allowing the solvent to evaporate from the surface and the lipid to equilibrate in the gaseous phase for at least 30 min. Areas were calculated from the movement of the barrier; surface pressures were read from the chart recorder trace.

2.4. Fluorescence anisotropy

Unilamellar vesicles of DMPC/POPA and DMPC/POPA/CF were prepared as described above. Steady-state fluorescence polarization measurements were obtained essentially as described by Litman and Barenholz [32]. Aliquots of vesicles were diluted to 0.1 A_{500} and incubated for 1 h at 30°C with a DPH:lipid mol ratio of 1:1000. Fluorescence emission intensities were obtained at 30°C on a Perkin-Elmer LS-5 fluorescence spectrometer equipped with a polarization accessory.

2.5. Fourier transform infrared spectroscopy (FTIR)

Multilamellar vesicles of DMPS, DMPS/CF, and DMPS/TEC-Mal were prepared as described above using 100 mM NaCl, 10 mM Tes at pH 7.4 or the same buffer with 10 mM $CaCl_2$. The samples were placed as a capillary film on the FTIR windows. Temperature of the sample was regulated by a Peltier device constructed by Paige Instruments (Davis, CA) and monitored by a thermocouple embedded in a cavity drilled in the upper window. Spectra were collected on a Perkin-Elmer 1750 FTIR (Perkin-Elmer, Norwalk, CT) and analyzed using Perkin-Elmer software. Center of gravity analysis of the CH_2 stretching vibrations was done as described by Cameron and Moffat [33]. The position of the PO_2 asymmetric stretch was determined by choosing the center of the peak absorbance. Although not constant as in a differential scanning calorimeter, the average heating rate during the temperature scans of these experiments was 30C°/h.

2.6. Membrane-associated water

The amount of membrane-associated water was determined by measuring the unfrozen water fraction of water : lipid samples, using differential scanning calorimetry. Multilamellar vesicles of DPPC, DPPC/TEC-Mal, DPPC/CF and DPPC/TDB were prepared as described above, at a water content in the range of 50–70% (w/w). Aliquots of the MLV (3–7 μl) were sealed in pre-weighed 15 μl aluminum pans and weighed to the nearest μg on a Cahn Electrobalance. Samples were scanned using a Perkin-Elmer DSC-2C differential scanning calorimeter cooled with an Infra-

Cooler II and data were collected and analyzed using Perkin-Elmer software.

The samples were cooled rapidly to −80°C and held there until equilibrated, then heated to the beginning of the ice melting peak (previously determined) and held for 1 h. The samples were again cooled to −80°C, equilibrated, and heated at 5 deg/min past the ice melting peak and lipid transition to check the homogeneity of the sample. Cooling scans (10 deg/min) of the same samples were recorded from 50 to −80°C. DPPC was chosen for these experiments since the lipid transition is well removed from the ice melt.

Following the scans, the pans were re-weighed to check for leaks, then punctured and dried for 24–36 h over anhydrous $CaSO_4$ at 60°C followed by 24–36 h under vacuum (1.33 Pa). The pans were removed from the lyophilizer under vacuum, removed from the flask in a dry box flushed with nitrogen at 10% relative humidity, and sealed in vials until just before weighing. The amount of unfrozen water/lipid was calculated from the measured and expected enthalpy of the ice melting peak, the water weight, and the dry weight of the lipid in the DSC pan.

2.7. Lipid phase transitions

The lipid phase transitions of the multilamellar vesicles used for membrane-associated water were also examined by differential scanning calorimetry using the same scans that were used to determine the ice melting or by FTIR.

3. Results and discussion

3.1. Monolayer films

Compression isotherms for monolayer films of POPA, DMPC, and CF are shown in Fig. 1. Since these data were collected at 30°C, above the gel-liquid crystalline transition of DMPC and POPA, the curves correspond to the fluid expanded phase of Durand et al. [34] with collapse pressures approaching 40 mN/m, consistent with previously reported values for DMPC [35–37] and CF [34,38]. The isotherm of C_{52} cord factor (C, in Fig. 1) is also a single smooth curve, thus this particular CF is also in a fluid expanded phase at this temperature. Additionally, curve C demonstrates that although it is not possible to hydrate bulk dry C_{52} CF or form liposomes from it (see below), it does form an ordered array when spread from solvent as a monomolecular film. Data from the gaseous phase of the compression isotherms (essentially zero) are omitted from Fig. 1 in order to present the curves more clearly.

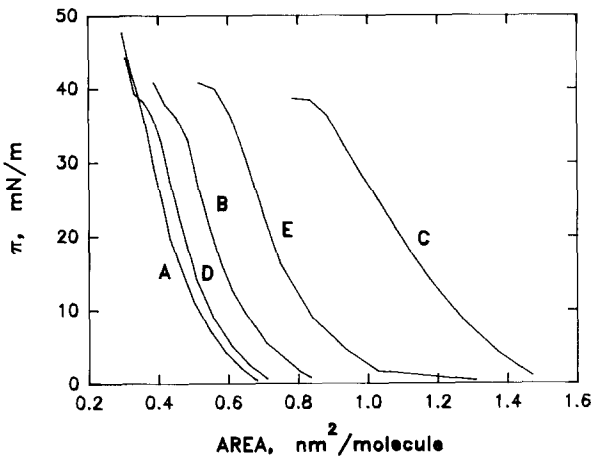

Fig. 1. Isothermal compressions of monolayer films of pure DMPC (A), POPA (B) and CF (C) and mixed monolayers of DMPC/POPA (D) at a 1:1 mol ratio and DMPC/POPA/CF (E) at a 1:1:0.1 mol ratio. Molecular areas are given in Table 1. Addition of a small amount of CF spreads the monolayer more than expected on the basis of the contributions of the individual lipids. Data from the compression of the gaseous phase (near zero surface pressure) have been omitted from the figure in order to provide a clearer presentation.

Although the area/molecule is commonly determined by extrapolation of the most condensed part of the compression isotherm to zero pressure [34], it is perhaps more meaningful to express the molecular area at a pressure which more realistically represents

Table 1
Observed and expected values for the molecular area (in nm^2/molecule) of pure and mixed monolayers of DMPC, POPA and CF

Lipid(s)	Observed area at zero pressure	Expected area at zero pressure	Observed area at 30 mN/m	Expected area at 30 mN/m
DMPC	0.51	–	0.39	–
POPA	0.65	–	0.51	–
CF	1.35	–	0.96	–
DMPC/POPA	0.57	0.58	0.43	0.45
DMPC/POPA/CF	0.84	0.62	0.67	0.47

Expected values of the molecular area of the mixed lipid monolayers were calculated using the observed molecular area for the pure lipid assuming no lipid-lipid interaction between lipid species. There is close agreement between the observed and expected values of the mixed DMPC/POPA (1:1 mol ratio) molecular areas, but the observed molecular area of the mixed monolayer containing DMPC/POPA/CF (1:1:0.1 mol ratio) is significantly larger than expected.

the pressure within a bilayer. Both determinations are presented in Table 1 in order to allow comparisons with literature values. Lipid mixtures of DMPC/POPA (1:1 mol ratio) and DMPC/POPA/CF (1:1:0.1 mol ratios) were cast to determine the effects of these mixtures on the spreading of the monolayer. Mixtures of DMPC/POPA resulted in an area/molecule of 0.43 nm^2 at 30 mN/m, intermediate between those for the pure phospholipids, as expected. However, the addition of 1 mol% of CF shifted the area/molecule to 0.67 nm^2, about 40% more than expected based on the contribution of each individual species in the mixture.

The observation that CF can spread a monolayer is not new. Using a cord factor with C_{80} dicyclopropane mycolic fatty acids and egg lecithin, Durand et al. [34] found that this CF expanded egg lecithin monolayers at all mol fractions at 20°C and 30 mN/m pressure. Both the egg lecithin and the cord factor are in the fluid expanded phase, as are the DPPC, POPA and C_{52} CF in the present study. Durand et al. [34] also found that a saturated C_{32} CF which showed a phase change during compression led to film condensation at several pressures and mol fractions. From the compression isotherm of dipalmitoyl trehalose, these authors conclude that the minimum molecular area for the trehalose ring at the interface is 0.55 nm^2, thus the increase in molecular area seen for fully compressed films of C_{32}, C_{52} and C_{80} cord factors must be due to the bulky, branched mycolic acids.

3.2. Membrane-associated water

In order to determine the degree to which CF affects the hydration of phospholipid membranes, the amount of water remaining unfrozen in frozen preparations was determined (Table 2). A measure of unfrozen water in membranes will indicate overall close association of water with the membrane, but not the type of association (i.e., bound to, restricted in motion or oriented by the membrane assembly). Nuclear magnetic resonance and DSC studies have estimated such water at 7–9 mol/mol lipid [39–41].

The calorimetric enthalpy of the ice melting peak was determined in MLV of DPPC, DPPC/CF, DPPC/TDB, and DPPC/TEC-Mal (9:1 mol ratio) and mol ratios of unfrozen water/lipid were calculated as described in Materials and methods. Cooling scans of these hydrated MLV showed that there are two water freezing events, a heterogeneous nucleation at approximately −19°C and a much smaller homogenous nucleation at −45°C. There is only one ice melting event on heating from −80°C. Homogeneous ice nucleation occurs in very small volumes of water [42] and the freezing event at −45 probably represents the water at the center of the multilamellar vesicles.

Table 2
Membrane-associated water, estimated from the unfrozen water of lipid/water samples

Lipid(s)	Mol water/mol total lipid
DPPC	7.2±0.1
DPPC/CF	10.9±0.2
DPPC/TDB	10.5±0.6
DPPC/TEC-Mal	11.1±0.4

Values are expressed as mol unfrozen water/mol total lipid, ±S.E, $n = 3$ separate samples. The three glycolipid-containing bilayers do not have signigicantly different amounts of membrane-associated water, but all are significantly more than pure DPPC.

According to our measurements, DPPC has approximately 7 mol water/mol lipid that do not freeze with the bulk water under these conditions, consistent with published values for water of hydration of DPPC determined by DSC [41]. Hydrated MLV made from mixtures of DPPC/CF, DPPC/TDB, and DPPC/TEC-Mal have an unfrozen water fraction equivalent to 11 mol/mol lipid, or about 50% more unfrozen water that pure DPPC. Pure CF had no unfrozen water, which is consistent with the fact that we were unable to hydrate a film of CF, even at 100°C, or to form sonicated vesicles, although sonicated dispersions of a *M. tuberculosis* cord factor have been reported [38]. Differential scanning calorimetry showed that the C_{52} CF which had been dried from chloroform in 15 μl pans and had a small amount of water added displayed only an ice-melting peak when run from −80 to 100°C and showed no homogeneous nucleation event. The enthalpy of the ice-melting peak matched the value expected from the weight of water in the pans. These results are not unexpected in view of reports reviewed in [43] and the large hydrophobic domain of C_{52} CF.

The data above indicate that there is more water associated with a mixed bilayer in the presence of CF, TEC-Mal, and trehalose dibehenate. This effect could be due to one of two mechanisms: (a) the presence of carbohydrate (which presumably hydrogen bonds water) in the headgroup region or (b) spreading of the bilayer by the hydrophobic portion, leading to increased access by water molecules to polar residues in the lipids. The fact that all three glycolipids increase the membrane-associated water despite the large differences in their hydrophobic portions suggests that the carbohydrate is the important factor in increasing headgroup hydration.

Differential scanning calorimetry of mixtures of the various glycolipids with DPPC (not shown) shows that they form homogeneous mixtures. All of the mixtures showed a single broadened transition when scanned to at least 90°C.

3.3. Fluorescence anisotropy

The association of water (or hydration) of the membrane may be important to our understanding of the

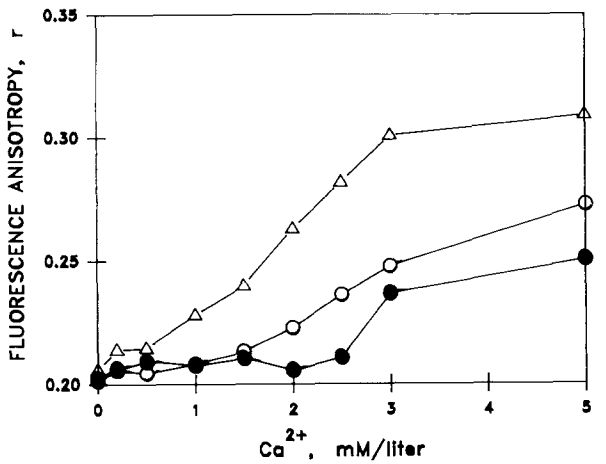

Fig. 2. Steady-state fluorescence anisotropy measurements, at 30°C, of unilamellar vesicles prepared from PS and PS/CF. The addition of Ca^{2+} to PS liposomes results in a marked increase in the anisotropy value (r) (△). PS/CF (9:1 mol ratio) liposomes (○) and 4:1 mol ratio liposomes (●) showed a less marked increase in r and only after the addition of 1.5 and 3.0 mM Ca^{2+}, respectively.

role CF plays in Ca^{2+}-induced fusion. Lucy [15,16] along with others [18–21,23] have developed models to explain the interaction of Ca^{2+} with acidic phospholipids as one which results in a dehydration of the lipid interface along with increased rigidity of the acyl chains. Gel phase lipid domains resulting from the interaction of Ca^{2+} with acidic phospholipids are thought to be important at the site of fusion in phospholipid vesicles and biological membranes [19,20]. FTIR and Raman spectroscopy have been used to study the interaction [25,44,45] and have shown that Ca^{2+} binds to the phosphate ester leading to a rigid, immobilized, partially hydrated structure of the headgroup region.

The effect of Ca^{2+} on the acyl chain behavior of an acidic bilayer is shown in Fig. 2. At 30°C, above the gel-to-liquid crystalline transition of PS, unilamellar vesicles of PS and PS/CF show increasing rigidity as measured by fluorescence anisotropy of DPH located in the hydrophobic domain of the vesicles. This fluorescent probe shows no preferential partitioning into gel or liquid crystalline domains [46], thus the anisotropy values report the fluidity of the whole bilayer. Addition of as little as 0.5 mM Ca^{2+} resulted in an increase in the anisotropy values for pure PS which rose steadily to 0.31 with the addition of Ca^{2+} up to 5 mM. This increase is indicative of an isothermal crystallization of the acyl chain region noted as the vesicles undergo a gel-to-liquid crystalline transition at 30°C. PS/CF LUV (9:1 mol ratio) showed decreased anisotropy compared to control vesicles at Ca^{2+} concentrations of 1 mM and higher. Doubling the CF concentration in the vesicles resulted in no increase in anisotropy until the addition of 3 mM Ca^{2+}, and was lower than the vesicles containing 10 mol% CF at Ca^{2+} concentrations of 2 mM and above. These data show that CF reduces the rigidification of acyl chains of PS in the presence of increasing amounts of Ca^{2+} but does not address the question of dehydration of the headgroup.

3.4. Fourier transform infrared spectroscopy

In order to obtain additional information about the effect of Ca^{2+} on both acyl chain rigidification and headgroup dehydration we used MLV of DMPS and mixtures of DMPS with CF, trehalose dibehenate and TEC-Mal. DMPS has a transition at 39°C as measured by differential scanning calorimetry [24] and FTIR [26] and thus is useful for examining changes in the chain-melting temperature. Our results are consistent with these earlier measurements and also show that this transition is unaffected by the addition of 10 mol% of CF (Fig. 3).

To determine the extent to which CF might reduce the Ca^{2+}-induced liquid crystalline-to-gel transition temperature, we measured the temperature-dependent change in the frequency of the symmetric CH_2 stretch of the multilayers in the presence of 10 mM Ca^{2+}. Earlier studies of bovine brain PS [25] or DMPS [24] showed that in excess Ca^{2+} the chain-melting transition is eliminated or shifted to extremely high temperatures. We have used a lower Ca^{2+}/DMPS ratio of approximately 1:2 which causes an increase in chain-melting temperature to approximately 65°C (Fig. 3).

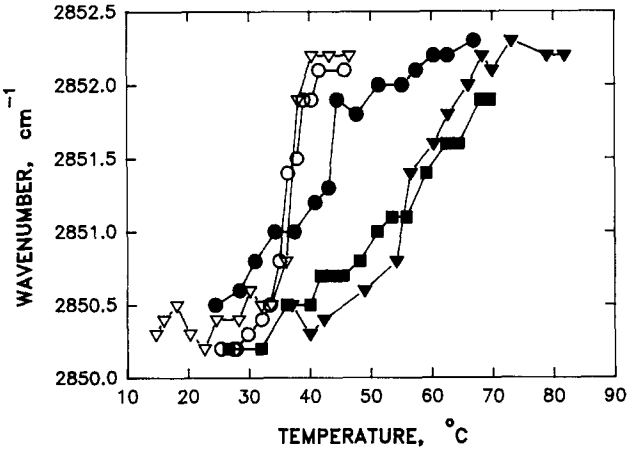

Fig. 3. Gel-to-liquid crystalline phase transitions of MLV of DMPS (▽), DMPS/CF (○), DMPS/CF plus 10 mM Ca^{2+} (●), DMPS plus 10 mM Ca^{2} (▼) and DMPS/TEC-Mal plus 10 mM Ca^{2+} (■) as measured by the change in the center of gravity of the CH_2 symmetric stretching vibration. T_m values are measured at the midpoint of the curve and were estimated to be approximately 36°C for DMPS and DMPS/CF. The effect of Ca^{2+} on these MLV is to shift the T_m to about 45°C for DMPS/CF and about 65°C for DMPS and DMPS/TEC-Mal. The scan of DMPS/TEC-Mal ended at 70°C due to failure of the temperature controller. Mixtures of DMPS with TEC-Mal and TDB in the absence of Ca^{2+} superimposed on the curve for pure DMPS, while addition of Ca^{2+} caused a shift of the transition of DMPS/TDB to above 65°C (data not shown).

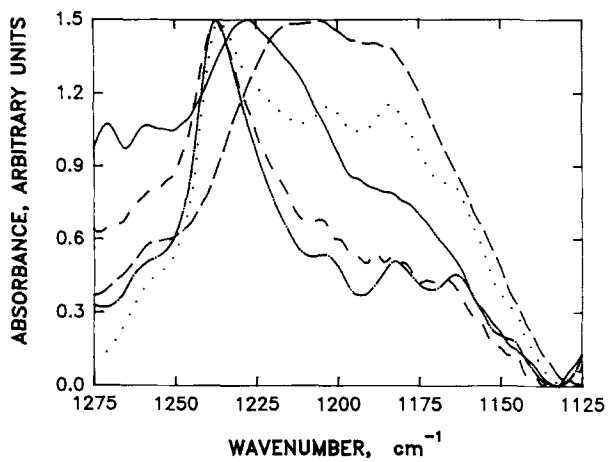

Fig. 4. Spectra of the asymmetric PO_2 stretch region at 30°C. All samples hydrated with 10 mM Ca^{2+} (including DMPS/TDB which is not shown) showed a dehydration of the phosphate group with peaks at about 1238 cm^{-1}. Pure DMPS and mixtures of DMPS with TEC-Mal and TDB all had a PO_2 stretch at about 1228 cm^{-1}. In the presence of CF, the PO_2 stretch is shifted downward from the pure DMPS peak, suggesting that the DMPS/CF bilayer is more highly hydrogen-bonded to water. DMPS in buffer, solid line; DMPS/CF in buffer, long dashed line; DMPS in Ca^{2+} buffer, medium dashed line; DMPS/CF in Ca^{2+} buffer, dash-and-dot line; DMPS/TEC-Mal in Ca^{2+} buffer, dotted line.

However, DMPS/CF MLV in the presence of Ca^{2+} have a chain-melting transition which is broadened, with a mid-point of approximately 43°C. The marked increase in T_m of DMPS in the presence of Ca^{2+} has been explained by the binding of Ca^{2+} to the PS headgroup, which causes dehydration of the phosphate and induces a liquid crystalline-to-gel transition [20, 24–26,44,45]. Clearly, a much less marked increase of the T_m of DMPS MLV is observed here when CF is incorporated in the bilayer.

Since the results using DPPC indicated that the incorporation of CF resulted in increased headgroup hydration, we recorded the spectra of the PO_2 asymmetric stretch of DMPS and DMPS/CF with and without Ca^{2+} to monitor its effects on headgroup hydration (Fig. 4) Consistent with previous results [23], hydrated DMPS has a PO_2 stretch at about 1228 cm^{-1}, indicative of extensive hydrogen bonding, while the same sample was clearly dehydrated in the presence of Ca^{2+}, with an increase of about 10–11 wavenumbers for the PO_2 asymmetric stretch. Despite the fact that the order-disorder transition of DMPS/CF as shown by the symmetric CH_2 stretch was only slightly affected by the presence of 10 mM Ca^{2+}, the headgroup of the DMPS in the DMPS/CF mixture was fully dehydrated by the Ca^{2+} as indicated by the shift of the PO_2 peak. In this mixture the DMPS contributed over 70% of the CH_2 groups, thus the transition seen represents both the DMPS and the CF. This is further confirmed by the fact that the total wavenumber change is approximately equal for all samples. The PO_2 stretch of the DMPS in the presence of CF was shifted to wavenumbers below 1210 cm^{-1}, consistent with data above which indicates increased hydration and molecular area in lipid mixtures containing CF.

MLV of DPPC/TEC-Mal and DPPC/TDB had an increase in headgroup hydration equal to that seen in MLV of DPPC/CF. To distinguish the effect of headgroup hydration from the effect of the mycolic acid chains on bilayer disorder, we looked at the CH_2 and PO_2 stretches of DMPS/TEC-Mal and DMPS/TDB MLV in the absence and presence of Ca^{2+}. In the absence of Ca^{2+}, the transition for both these mixtures overlaid the transitions for pure DMPS and DMPS/CF, again indicating a homogeneous mixture. However, although TEC-Mal and trehalose dibehenate increase headgroup hydration as much as CF in DPPC mixtures, they were unable to prevent an increase in the temperature of the order-disorder transition of the CH_2 groups of DMPS in the presence of Ca^{2+} or the dehydration of the DMPS headgroup. Thus, the mycolic acid chains of the CF are important in maintaining bilayer fluidity in the presence of Ca^{2+}.

It is possible that in addition to the role of the mycolic acid chains in maintaining bilayer fluidity, the increased hydration resulting from the presence of CF in the bilayer may provide some steric hindrance to the close approach of membranes which is a prerequisite to fusion. The increased hydration of the membrane in the presence of CF (as demonstrated by the DSC measurements of membrane-associated water) may contribute to the inhibition of Ca^{2+}-induced fusion by increasing the hydration barrier to fusion (for reviews see [28,47]), especially in lipid mixtures with lower PS content. The increased hydration of the bilayer surface in the presence of CF could act in two ways: (1) by reducing the likelihood that physiological concentrations of Ca^{2+} will dehydrate the membrane surface and allow Ca^{2+} bridge formation between opposing membranes and (2) by producing hydration forces at the bilayer surface which act to prevent the close approach of membranes necessary for fusion.

4. Conclusions

The data in this paper demonstrate that CF increases both the molecular area of phospholipids in a monolayer and the amount of water closely associated with bilayers of phospholipids. The fluidity of membranes containing cord factor and an acidic phospholipid is maintained in the presence of Ca^{2+} despite the dehydration of the headgroup by the calcium ion. Since cord factor does not bind Ca^{2+} and dehydrate, there is a population of bulky mycolic acid chains in the bilayer which do not rigidify and thus maintain bilayer fluidity.

This may be the most important factor which accounts for the decreased fusion between cord factor containing liposomes.

It is also possible that increased headgroup hydration may contribute to the inhibition of fusion by the cord factor by increasing hydration forces between membranes. We are presently pursuing these possibilities with the use of other naturally occurring cord factor analogues with different sugar headgroups and hydrophobic domains of different sizes combined in lipid mixtures of more realistic composition than pure DMPS.

Acknowledgements

We gratefully acknowledge the support of this work by grants DCB-89-18822 from the National Science Foundation to J.H.C. and L.M.C., 2RO1-AI20900 and 5RO1-AI20900-8 from the National Institute of Allergy and Infectious Disease to B.L.B., and a University of California Jastro-Shields Research Fellowship to B.J.S.

References

[1] Armstrong, J.A. and Hart, P.D. (1971) J. Exp. Med. 134, 713–740.
[2] Goren, M.B., Hart, P.D., Young, M.R. and Armstrong, J.A. (1976) Proc. Natl. Acad. Sci. USA 73, 2510–2514.
[3] Davis-Scibienski, C. and Beaman, BL. (1971) Infect. Immun. 29, 24–29.
[4] Goren, M.B., Swendsen, C.L., Fiscus, J. and Miranti, C. (1984) J. Leuk. Biol. 36, 273–292.
[5] Frehel, C., De Chastellier, C., Lang, T. and Rastogi, N. (1986) Infect. Immun. 52, 252–262.
[6] Hart, P.D., Young, M.R., Gordon, A.H. and Sullivan, K.H. (1987) J. Exp. Med. 166, 933–946.
[7] De Chastellier, C., Frehel, C., Offredo, C. and Skamene, E. (1993) Infect. Immun. 61, 3775–3784.
[8] Goren, M.B., Vatter, A.E. and Fiscus, J. (1987) J. Leuk. Biol. 41, 122–129.
[9] Hart, P.D. and Young, M.R. (1988) J. Leuk. Biol. 43, 179–182.
[10] Goren, M.B. (1970) Biochim. Biophys. Acta 120, 116–126.
[11] Sturgill-Koszycki, S., Schlesinger, P.S., Chakraborty, P., Haddix, P.L., Collins, H.L., Fok, A.K., Allen, R.D., Gluck, S.L., Heuser, J. and Russell, D.G. (1994) Science 263, 678–681.
[12] Black, C.M., Paliescheskey, M., Beaman, B.L., Donovan, R.M. and Goldstein, E. (1986) J. Infect. Dis. 154, 952–958.
[13] Ioneda, T., Beaman, B.L., Viscaya, L. and Almeida, E.T. (1993) Chem. Phys. Lipids 65, 171–178.
[14] Ioneda, T. and Beaman, B.L. (1992) Chem. Phys. Lipids 63, 41–46.
[15] Spargo, B.J., Crowe, L.M., Ioneda, T., Beaman, B.L. and Crowe, J.H. (1991) Proc. Natl. Acad. Sci. USA 88, 737–740.
[16] Lucy, J.A. (1970) Nature 227, 814–817.
[17] Lucy, J.A. (1984) In Membrane Processes (Benga, G., Baum, H. and Kummerow, F.A., eds.), pp. 27–48, Springer-Verlag, New York.
[18] Wilschut, J. and Hoekstra, D. (1984) Trends Biochem. Sci. 9, 479–483.
[19] Papahadjopoulos, D., Vail, W.G., Pangborn, W.A. and Poste, G. (1976) Biochim. Biophys. Acta 448, 265–283.
[20] Papahadjopoulos, D., Poste, G. and Vail, W.G. (1978) In Methods in Membrane Biology (Korn, E., ed.), Plenum Press, New York.
[21] Düzgünes, N., Wilschut, J., Fraley, R. and Papahadjopoulos, D. (1979) Biochim. Biophys. Acta 642, 182–195.
[22] Portis, A., Newton, C., Pangborn, W. and D. Papahajopoulos, D. (1979) Biochemistry 18, 780–790.
[23] Casal, H.L., A. Martin, A., Mantsch, H.H., Paltauf, F. and Hauser, H. (1987) Biochemistry 26, 7395–7401.
[24] Hauser, H. and Shipley, G.G. (1984) Biochemistry 23, 34–41.
[25] Dluhy, R.A., Cameron, D.G., Mantsch, H.H. and Mendelsohn, R. (1983) Biochemistry 22, 6318–6325.
[26] Casal, H.L., Mantsch, H.H. and Hauser, H. (1987) Biochemistry 26, 4408–4416.
[27] Wilschut, J. (1991) In Membrane Fusion (Wilschut, J. and Hoekstra, D., eds.), pp. 89–126, Marcel Dekker, New York.
[28] Israelachvili, J.N. (1985) In Intermolecular and Surface Forces (Israelachvili, J.N., ed.), pp. 265–275, Academic Press, London.
[29] Goodrich, R.P., Crowe, J.H., Crowe, L.M. and Baldeschweiler, J.D. (1991) Biochemistry 30, 5313–5318.
[30] Kates, M. (1986) Techniques of Lipidology, Elsevier, Amsterdam.
[31] Deamer, D.W. (1978) In Liposome Technology, Volume I: Preparation of Liposomes (Gregoriadis, G., ed.), CRC Press, Boca Raton.
[32] Litman, B.J. and Barenholz, Y. (1982) Methods Enzymol. 81, 678–685.
[33] Cameron, D.G. and Moffatt, D.L. (1984) J. Test. Eval. 12, 78–85.
[34] Durand, E., Welby, M., Laneelle, G. and Tocanne, J.-F. (1979) Eur. J. Biochem. 93, 103–112.
[35] Van Deenen, L.L.M., Houtsmuller, U.M.T., De Haas, G.H. and Mulder (1962) J. Pharm. Pharmacol. 14, 429–444.
[36] Horn, L.W. and Gershfeld, N.L. (1977) Biophys. J. 18, 301–310.
[37] Rudolph, A.R., Crowe, J.H. and Crowe, L.M. (1986) Arch. Biochem. Biophys. 245, 134–143.
[38] Retzinger, G.S., Meredith, S.C., Takayama, K., Hunter, R.L. and Kédzy, F.J. (1981) J. Biol. Chem. 256, 8208–8216.
[39] Finer, E.G. and Darke, A. (1974) Chem. Phys. Lipids 12, 1–16.
[40] Salsbury, N.J., Darke, A. and Chapman, D. (1972) Chem. Phys. Lipids 8, 142–151.
[41] Bronshteyn, V.L. and Steponkus, P.L. (1991) Cryobiology 28, 530–531.
[42] Charoenrein, S. and Reid, D.S. (1989) Thermochim. Acta 156, 373–381.
[43] Asselineau, C. and Asselineau, J. (1978) Prog. Chem. Fats Other Lipids 16, 59–99.
[44] Hark, S.K. and Ho, J.T. (1979) Biochem. Biophys. Res. Commun. 91, 665–670.
[45] Hark, S.K. and Ho, J.T. (1980) Biochim. Biophys. Acta 601, 54–62.
[46] Lentz, B.R., Barenholz, Y. and Thompson, T.E. (1976) Biochemistry 15, 4529–4536.
[47] Sundler, R. (1984) In Biomembranes, Volume 12, Membrane Fluidity (Kates, M. and Manson, L.A., eds.), Plenum Press, New York.